

Current Biology, Volume 29

Supplemental Information

Microtubule End-Clustering

Maintains a Steady-State Spindle Shape

Christina L. Hueschen, Vahe Galstyan, Meelad Amouzgar, Rob Phillips, and Sophie Dumont

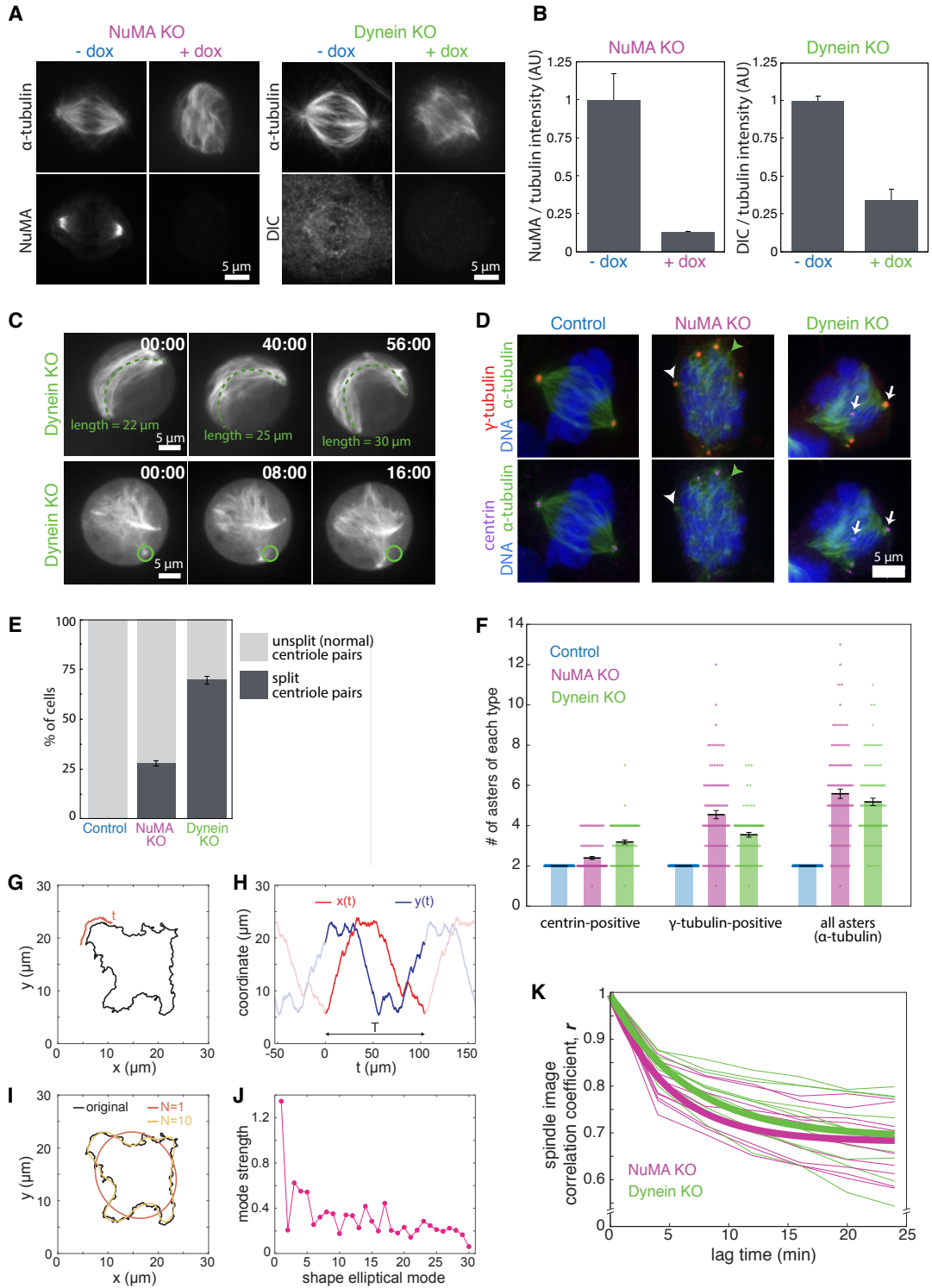


Figure S1. Validation and additional analysis of NuMA and dynein knockout.

Related to Figure 1. (A) Representative immunofluorescence images of mitotic cells in which NuMA or dynein heavy chain has been knocked out by an inducible CRISPR-Cas9 system.

Dynein intermediate chain (DIC) depletion has been shown to correlate with dynein heavy chain depletion [S1]. (B) Quantification of NuMA or DIC intensity in sum projection immunofluorescence images, normalized to tubulin intensity. Bars show mean \pm SEM; n=20 cells each condition. Whenever possible, complete NuMA or dynein loss within individual cells analyzed was verified by immunofluorescence or by spindle morphology. (C) Time-lapse live images of dynein knockout (KO) spindles in human RPE1 cells stably expressing GFP-tubulin. These examples highlight two common features of turbulent spindles: motile asters and extending microtubule bundles – and bundles of bundles – that bend against the cell cortex. Green circle is a fiducial mark showing initial aster position. (D) Representative immunofluorescence images of NuMA and dynein KO spindles show that asters in turbulent spindles do not always contain centrioles (see white arrowhead for example; centrioles are labeled with centrin). Asters usually contain γ -tubulin (white arrowhead) but not always (green arrowhead). In knockout cells, pairs of centrioles sometimes split apart (arrows). (E-F) Quantification of (E) centriole pair splitting and (F) number of asters of each type in 125 control spindles, 106 NuMA KO spindles, and 100 dynein KO spindles from 3 independent experiments. (G-J) Elliptical Fourier analysis of spindle shapes. Also see Methods. (G) An example contour of a NuMA KO spindle. The red curve indicates the positional coordinate t along the contour. (H) The x- and y-projections of the contour in (G), parametrized with a position variable along the contour (t). Transparent curves represent the periodic extensions of the single period with total contour length T . (I) Fourier reconstructions of the spindle contour using $N = 1$ (red) and $N = 10$ (yellow) harmonics. (J) Elliptical Fourier mode strength spectrum of the contour in (G). (K) Exponential decay fits (thick lines) of spindle shape correlation coefficient (r) vs. lag time (thin lines are individual cells), from Figure 1E, using $r = a * e^{(-\frac{1}{\tau}) * lag\ time} + b$. For NuMA and dynein KO spindles, r decayed exponentially to a value of b

$=0.68\pm0.02$ (NuMA KO) and $b = 0.69\pm0.03$ (dynein KO). Conceptually, the value of b represents the lowest shape correlation (maximal shape change) achievable by turbulent spindles over any length of time. Correlation coefficients near zero are not possible, as they would essentially require the disappearance of the spindle. Decay lifetimes (τ) were 5.0 ± 0.2 min for NuMA KO and 6.8 ± 0.5 min for dynein KO. $a = 0.31\pm0.02$ for NuMA KO; $a = 0.30\pm0.03$ for dynein KO. $n=10$ cells each condition.

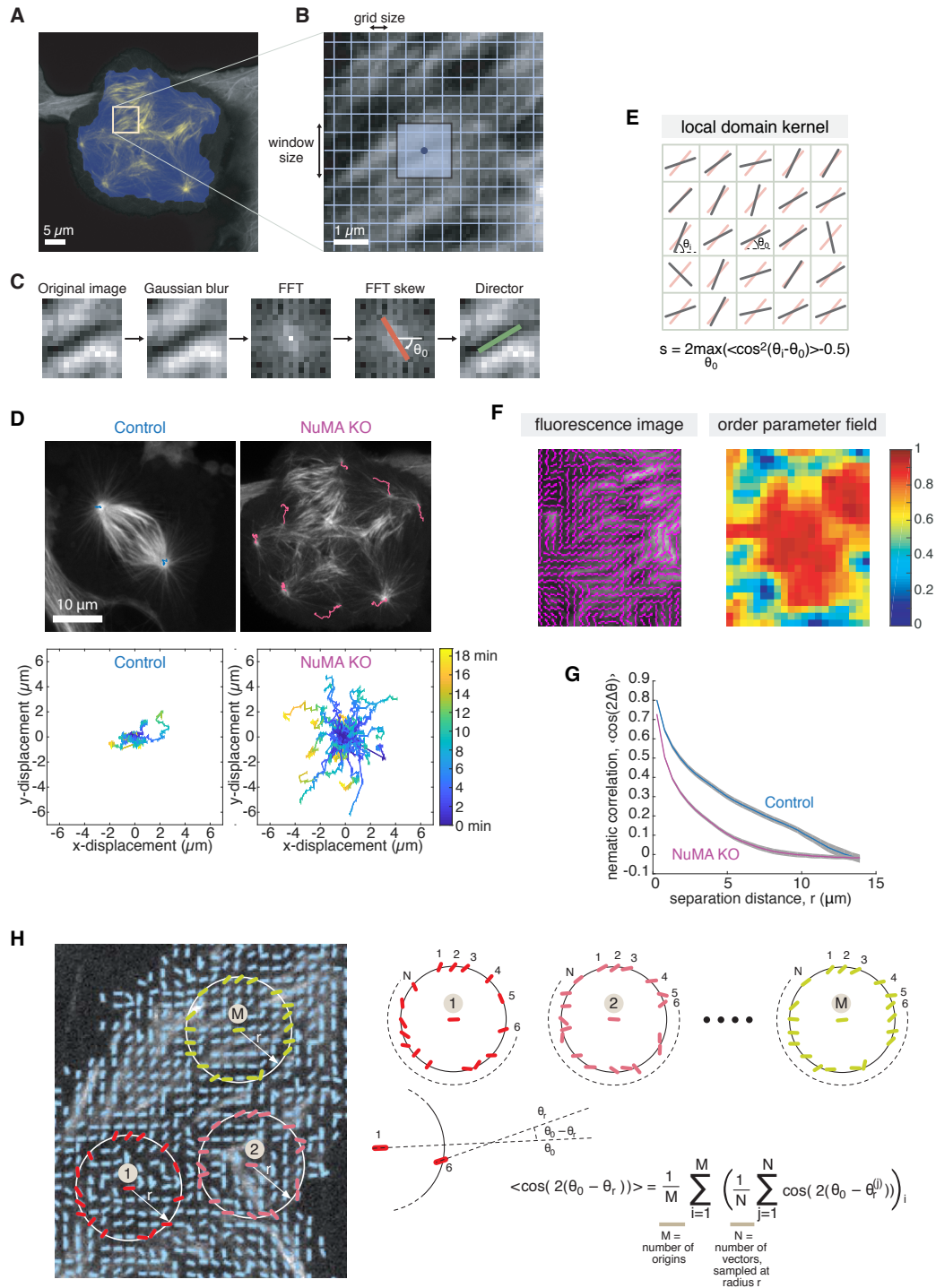


Figure S2. Nematic director field, order parameter, and correlation analyses.

Related to Figure 3. (A-C) Nematic director field extraction methodology. (A) NuMA KO spindle (transparent blue region) isolated in the fluorescence image based on intensity values. (B)

Grid of locations where the nematic director is evaluated using the pixel information in the image window centered at each grid point (transparent region). (C) Series of steps in director extraction. First, the Gaussian blur of the image window is taken. Second, the FFT is calculated (shown is the logarithm of FFT magnitudes, brighter pixels correspond to larger magnitudes). Third, principle skew direction of the transform, θ_0 , is obtained. Fourth, the local director perpendicular to the FFT skew direction is identified. (D) Tracks of aster position in control and NuMA KO spindles. In example images (top), 20 min tracks are overlaid on the first video frame. Below, 12 aster tracks from control spindles and 60 aster tracks from NuMA KO spindles are aligned to start at (0,0). Track color indicates time. (E-F) Nematic order parameter calculation. (E) Local domain of directors used to estimate the local order parameter at the central position. Dark line segments correspond to local directors (θ_i), and orange line segments correspond to the effective director of the domain (θ_0) that maximizes $s(\theta_0)$. (F) An example fluorescence image of a local region of the NuMA KO spindle shown in (A), along with the corresponding local nematic order parameter field. Red and blue coloring indicate high to low levels of local alignment. (G) Two-point spatial nematic correlation of microtubule orientation, $\langle \cos 2(\theta_r - \theta_0) \rangle$ as a function of separation distance, as illustrated in (H). (H) Schematic of spatial nematic correlation calculation. For each pair of directors \mathbf{n}_0 (at center of circle) and \mathbf{n}_r (along circle of radius r) within the spindle, we calculated $\cos 2(\theta_r - \theta_0)$ and binned by distance between 0 and r , then averaged over all possible pairs of directors.

SUPPLEMENTAL REFERENCES

- S1. Levy, J.R., and Holzbaur, E.L. (2008). Dynein drives nuclear rotation during forward progression of motile fibroblasts. *J Cell Sci* 121, 3187-3195.